

Organic dyes containing oligo-phenothiazine for dye-sensitized solar cells†

Yuan Jay Chang,^{*a} Po-Ting Chou,^b Yan-Zuo Lin,^c Motonori Watanabe,^d Chih-Jen Yang,^d Tsung-Mei Chin^c and Tahsin J. Chow^{*bd}

Received 15th July 2012, Accepted 29th August 2012

DOI: 10.1039/c2jm35556f

A series of organic dyes containing oligo-phenothiazine were synthesized and used effectively on the fabrication of dye-sensitized solar cells (DSSCs). In these compounds the phenothiazine moiety functions both as an electron donor and as a π -bridge. These materials exhibit considerably high values of open-circuit voltage (V_{oc}) ranging from 0.78–0.83 V under an AM1.5 solar condition (100 mW cm^{-2}). Two kinds of substituents, *i.e.*, hexyl and hexyloxyphenyl groups, were added onto the N(10) of phenothiazine for comparison. The best device displayed a short-circuit current (J_{sc}) of 14.3 mA cm^{-2} , an open-circuit voltage (V_{oc}) of 0.83 V, a fill factor (FF) of 0.65, corresponding to an overall conversion efficiency of 7.78%. Their photophysical properties were analyzed with the aid of a time-dependent density functional theory (TDDFT) model with the B3LYP functional. The electronic nature of the devices was further elucidated by using electrochemical impedance spectroscopy.

Introduction

The increased consumption of fossil and the more serious crisis of environment pollution have led us to the search for new and renewable energy sources. Solar energy is widely recognized as the most promising candidate to help solving this problem. Dye-sensitized solar cells (DSSCs) are expected to be potential tools due to their low cost processing and impressive photovoltaic performance.¹ The ruthenium-based dyes, reported by Michael Grätzel, have achieved maximal power conversion efficiencies over 11%. Yet they have encountered some problems, such as limited resources, elaborated purification processes, *etc.*² Compared with the rare and expensive metal complexes, organic dyes have the advantages of environmental friendliness, higher structural flexibility, lower cost, generally high molar extinction coefficients, easier preparation and purification, *etc.* Metal-free organic dyes have been widely investigated recently, many of which exhibited an energy-to-electricity conversion efficiency close to that of N719.^{3–6}

In the design of organic dyes for sensitized solar cells, it is critical to improve not only the value of the short-circuit current (J_{sc}) but also the value of the open-current voltage (V_{oc}). For the former it is necessary to improve the π -conjugation, so that the organic chromophore can harvest light energy to the largest extent. For the latter an effort of reducing the rate of charge recombination is necessary, so that the current leakage can be minimized. In our previous investigations, we have discovered that it is possible to use non-conjugated π -chromophores for DSSCs, *i.e.*, by incorporating a unit of paracyclophene to interrupt the π -system.⁷ The V_{oc} value of these materials can indeed reach a high standard as a result of slow rate of charge recombination. However, the relatively small value of J_{sc} became a drawback, due to the breaking down of the π -conjugation.

In this report we try to re-examine our concept by using phenothiazine as a building block. Phenothiazine contains electron-rich nitrogen and sulfur heteroatoms in the central ring, yet it is not fully conjugated in a classical sense. The geometry of the molecule is not planar, but slightly bent in the central ring. We envisioned that the non-planar conformation of phenothiazine can reduce not only the rate of charge recombination but also the molecular aggregation. The electron rich nature of a phenothiazine makes it a good electron donor during a photo-excited charge transfer transition. It displays a low and reversible oxidation potential toward the formation of a stable radical cation.^{8–11} By linking more than one unit of phenothiazine, we can examine the effect of chain length on the performance of DSSCs.

Three types of compounds composed of phenothiazine units are prepared, *i.e.*, **PT1**, **PT2**, and **PT3**, as shown in Fig. 1. The nitrogen atoms in each type of compounds are substituted by two kinds of linear chains, *i.e.*, derivatives **a** and **b**. A cyanoacrylate

^aDepartment of Chemistry, Tung Hai University, Taichung 407, Taiwan. E-mail: jaychang@thu.edu.tw; Fax: +886-4-23590426; Tel: +886-4-23590428 extn 305

^bDepartment of Chemistry, National Taiwan University, No.1, Sec. 4, Roosevelt Rd., Da'an Dist., Taipei 10617, Taiwan. E-mail: chowtj@gate.sinica.edu.tw; Fax: +886-2-27884179; Tel: +886-2-27898552

^cDepartment of Chemistry, Chinese Culture University, 55 Hwa Kang Rd, Yang-Ming Shan, Taipei 111, Taiwan

^dInstitute of Chemistry, Academia Sinica, No.128, Sec. 2, Academia Rd., Nankang Dist., Taipei 11529, Taiwan

† Electronic supplementary information (ESI) available: Experimental data (**PT1**, **PT2** and **PT3**), the ¹H and ¹³C NMR spectra, theoretical calculation, UV/vis spectra, CV spectra, and EIS spectra, and the devices incorporating DCA. See DOI: 10.1039/c2jm35556f

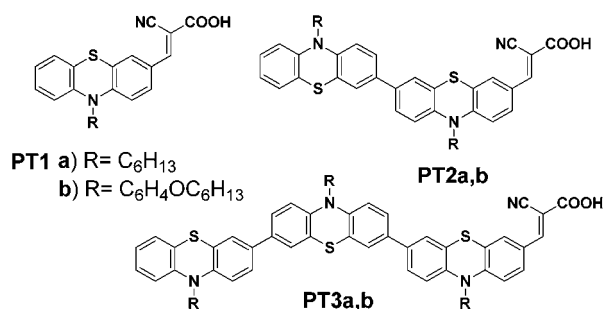


Fig. 1 Organic dye structures of oligo-phenothiazine.

group is attached to one side of the compound, acting as an electron acceptor. The synthetic procedures of **PT1**, **PT2**, and **PT3** are described in Scheme 1. All structures were confirmed by their spectroscopic data.

Experimental

General information

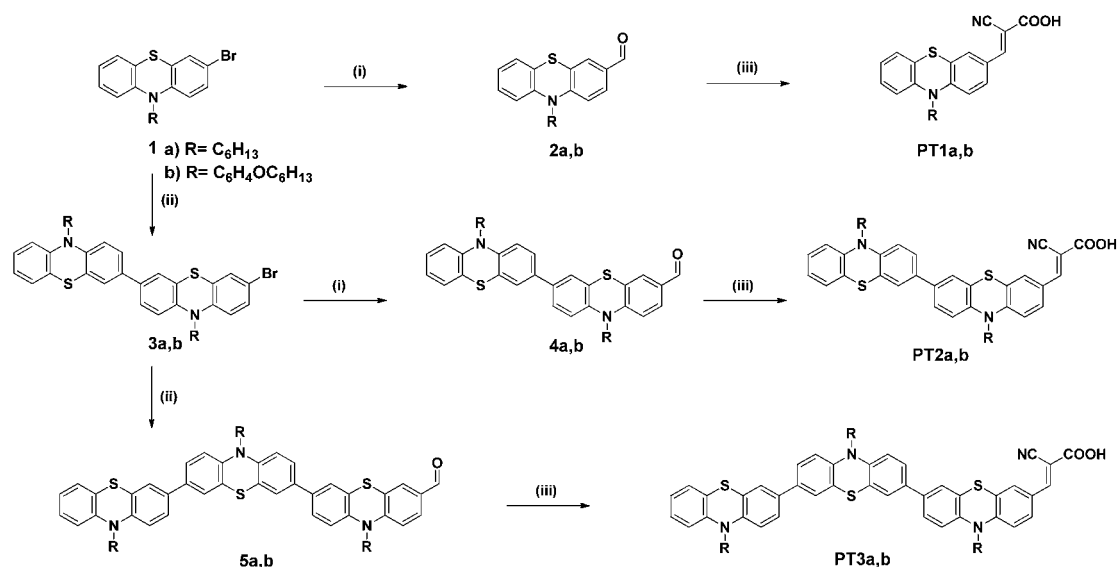
All reactions and manipulations were carried out under a nitrogen atmosphere. Solvents were distilled freshly according to standard procedures. ¹H and ¹³C NMR spectra were recorded on a Bruker (AV 400/AV 500 MHz) spectrometer in CDCl₃ and DMSO-d₆ as solvents. Chemical shifts are reported in δ scale downfield from the peak for tetramethylsilane. Absorption spectra were recorded on a Jasco-550 spectrophotometer. Emission spectra were obtained from a Hitachi F-4500 spectrofluorimeter. The emission spectra in solutions were measured in a spectral grade solvent using a 90° angle detection. The redox potentials were measured by using cyclic voltammetry on a CHI 620 analyzer. All measurements were carried out in THF

solutions containing 0.1 M tetrabutylammonium hexafluorophosphate (TBAPF₆) as supporting electrolyte under ambient conditions after purging for 10 minutes with N₂. The conventional three-electrode configuration was employed, which consists of a glassy carbon working electrode, a platinum counter electrode, and a Ag/Ag⁺ reference electrode calibrated with ferrocene/ferrocenium (Fc/Fc⁺) as an internal reference. Mass spectra were recorded on a VG70-250S mass spectrometer.

The chemicals, *i.e.*, phenothiazine, 4-bromophenol, 1-bromohexane, butyllithium (1.6 M in hexane), tetrakis(triphenylphosphine) palladium (Pd(PPh₃)₄), *N,N*-dimethylformamide, triisopropylborate, palladium(II) acetate (Pd(OAc)₂), 1,1'-bis(diphenylphosphanyl)ferrocene (dppf), *N*-bromosuccinimide (NBS), cyanoacetic acid, ammonium acetate, and acetic acid, were purchased from ACROS, Alfa, Merck, Lancaster, TCI, Showa, and Sigma-Aldrich, separately. Chromatographic separations were carried out by using silica gel from Merk, Kieselgel si 60 (40–63 μm).

Fabrication and characterization of DSSCs

The FTO conducting glass (FTO glass, fluorine doped tin oxide over-layer, transmission >90% in the visible, sheet resistance 8 Ω per square), titania oxide pastes of Ti-nanoxide T/SP and Ti-nanoxide R/SP were purchased from Solaronix. A thin film of TiO₂ (16–18 μm) was coated on a 0.25 cm² FTO glass substrate. It was immersed in a THF solution containing 3 × 10⁻⁴ M dye sensitizers for at least 12 h, then rinsed with anhydrous acetonitrile and dried. Another piece of FTO sputtered with 100 nm thick Pt was used as a counter electrode. The active area was controlled at a dimension of 0.25 cm² by adhering 60 μm thick polyester tape on the Pt electrode. The photocathode was placed on top of the counter electrode and was tightly clipped together to form a cell. Electrolyte was then injected into the seam



Scheme 1 Synthetic route of organic dyes. *Reagents and conditions:* (i) *n*-BuLi, DMF, THF, -78 °C; (ii) (a) *n*-BuLi, triisopropylborate, THF, followed by HCl(aq), (b) Pd(PPh₃)₄, 3,7-dibromo-10-hexyl-10*H*-phenothiazine or 3,7-dibromo-10-(4-(hexyloxy)phenyl)-10*H*-phenothiazine (3) and 7-bromo-10-hexyl-10*H*-phenothiazine-3-carbaldehyde or 7-bromo-10-(4-(hexyloxy)phenyl)-10*H*-phenothiazine-3-carbaldehyde (5), toluene-THF (2/1), K₂CO₃ (2 M); and (iii) cyanoacetic acid, NH₄OAc, AcOH, 90–100 °C.

between two electrodes. An acetonitrile solution containing LiI (0.5 M), I₂ (0.05 M) and 4-*tert*-butylpyridine (TBP) (0.5 M) was used as the electrolyte 1 (E1). A solution of 3-dimethylimidazolium iodide (1.0 M), LiI (0.05 M), I₂ (0.03 M), guanidinium thiocyanate (0.1 M), and TBP (0.5 M) in MeCN : valeronitrile (85 : 15, v/v) was used as electrolyte 2 (E2). Devices made of a commercial dye N719 under the same conditions (3×10^{-4} M, Solaronix S.A., Switzerland) were used as reference. The cell parameters were obtained under incident light with an intensity of 100 mW cm⁻² measured by a thermopile probe (Oriol 71964), which was generated by a 300 W (Oriol Class A Solar Simulator 91160A-1000, Newport) passing through an AM 1.5 filter (Oriol 74110). The light intensity was further calibrated by an Oriol reference solar cell (Oriol 91150) and adjusted to be 1.0 sun. The monochromatic quantum efficiency was recorded through a monochromator (Oriol 74100) under short-circuit conditions. Electrochemical impedance spectra of DSSCs were recorded by an Impedance/Gain-Phase analyzer (SI 1260, Solartron).

N-Hexylphenothiazine-3-carbaldehyde (**2a**)

To a solution of 3-bromo-10-hexyl-10*H*-phenothiazine (2.0 g, 5.52 mmol) in THF at -78 °C was added dropwise *n*-BuLi (5.2 mL, 8.28 mmol, 1.6 M in hexane). The mixture was stirred for 1 h, then to it was added DMF (0.63 mL, 8.28 mmol). The reaction was stirred with a magnetic bar for 6 h, then was quenched by adding water, then was extracted with ethyl acetate. The organic layer was dried over anhydrous MgSO₄ and concentrated under reduced pressure to give the crude product. The product was purified by a silica gel column chromatograph eluted with dichloromethane-hexane (1/1). A yellow solid of **2a** was obtained in 80% yield (1.37 g, 4.41 mmol). Spectroscopic data of **2a**: δ_H (400 MHz, CDCl₃) 9.78 (s, 1H), 7.62 (dd, 1H, *J* = 1.9, 8.4 Hz), 7.56 (d, 1H, *J* = 1.8 Hz), 7.13–7.17 (m, 1H), 7.09 (dd, 1H, *J* = 1.3, 7.6 Hz), 6.95 (t, 1H, *J* = 7.5 Hz), 6.86–6.89 (m, 2H), 3.87 (t, 2H, *J* = 7.2 Hz), 1.76–1.83 (m, 2H), 1.39–1.46 (m, 2H), 1.29–1.31 (m, 4H), 0.87 (t, 3H, *J* = 7.0 Hz); δ_C (100 MHz, CDCl₃) 189.9, 150.7, 143.4, 131.0, 130.0, 128.3, 127.5, 125.0, 123.7, 123.5, 115.9, 114.7, 48.0, 31.3, 26.7, 26.5, 22.5, 13.9; MS (FAB, 70 eV): *m/z* (relative intensity) 311 (M⁺, 100); HRMS calcd for C₁₉H₂₁NOS: 311.1344, found 311.1341.

10-(4-(Hexyloxy)phenyl)-10*H*-phenothiazine-3-carbaldehyde (**2b**)

Compound **2b** was synthesized according to the same procedure as that of **2a**. A light yellow solid of **2b** was obtained in 77% yield. δ_H (400 MHz, CDCl₃) 9.69 (s, 1H), 7.45 (d, 1H, *J* = 1.6 Hz), 7.28 (dd, 1H, *J* = 8.2, 2.0 Hz), 7.27 (d, 2H, *J* = 8.8 Hz), 7.13 (d, 2H, *J* = 8.8 Hz), 6.96 (dd, 1H, *J* = 5.6, 3.6 Hz), 6.84 (dd, 2H, *J* = 5.8, 3.6 Hz), 6.22 (d, 1H, *J* = 8.8 Hz), 6.17–6.19 (m, 1H), 4.05 (t, 2H, *J* = 6.4 Hz), 1.84–1.88 (m, 2H), 1.51–1.55 (m, 2H), 1.38–1.42 (m, 4H), 0.93–0.97 (m, 3H). δ_C (100 MHz, CDCl₃) 189.6, 159.2, 149.5, 142.8, 132.0, 131.6, 130.9, 129.9, 127.3, 127.1, 126.6, 123.5, 120.0, 118.9, 116.7, 116.4, 115.0, 68.4, 31.5, 29.2, 25.7, 22.6, 14.0. MS (FAB, 70 eV): *m/z* (relative intensity) 404 ((M + H)⁺, 100); HRMS calcd for C₂₅H₂₅NO₂S: 404.1684, found 404.1694.

3-(3-Bromo-10-hexyl-10*H*-phenothiazin-7-yl)-10-hexyl-10*H*-phenothiazine (**3a**)

To a three-necked round-bottom flask containing **1a** (3.2 g, 8.83 mmol) was added dropwise BuLi (8.3 mL, 13.3 mmol, 1.6 M in hexane) in dry THF at -78 °C, after then the solution was brought up to 0 °C and was stirred by a magnetic bar for 30 minutes. The solution was cooled again to -78 °C and to it was added dropwise triisopropyl borate (3.6 mL, 13.3 mmol). The reaction mixture was warmed up gradually to room temperature and was stirred overnight. To the reaction mixture was then added an excess amount of 10% HCl_(aq) (30 mL), while the mixture was stirred for another 1 h. The reaction was quenched by pouring into distilled water, followed by extraction with ethyl acetate. The organic layer was dried over anhydrous MgSO₄. Evaporation of the solvent gave a crude product, which was immediately subjected to the next reaction. It was mixed with 3,7-dibromo-10-hexyl-10*H*-phenothiazine (3.89 g, 8.83 mmol), K₂CO_{3(aq)} (2.76 g, 2 mmol) in 10 mL H₂O, and Pd(PPh₃)₄ (310 mg, 0.26 mmol) in dry toluene-THF (2/1). The mixture was heated to 60 °C for 12 h. After cooling, the products were extracted with ethyl acetate and the organic layer dried over anhydrous MgSO₄. The crude product was dried *in vacuo*, and was purified using a silica gel column chromatograph eluted with CH₂Cl₂-hexane (1/1). A yellow solid of **3a** was obtained in 55% yield (3.12 g, 4.85 mmol). δ_H (400 MHz, CDCl₃) 7.20–7.33 (m, 6H), 7.18 (d, 2H, *J* = 7.2 Hz), 6.95 (t, 1H, *J* = 7.2 Hz), 6.89 (d, 2H, *J* = 9.2 Hz), 6.87 (d, 1H, *J* = 8.8 Hz), 6.70 (d, 1H, *J* = 8.4 Hz), 3.87 (t, 2H, *J* = 7.2 Hz), 3.81 (t, 2H, *J* = 7.2 Hz), 1.77–1.89 (m, 4H), 1.43–1.50 (m, 4H), 1.34–1.37 (m, 8H), 0.91–0.95 (m, 6H). δ_C (100 MHz, CDCl₃) 145.0, 144.3, 143.7, 134.6, 134.0, 129.9, 129.6, 127.4, 127.2, 126.7, 125.4, 125.2, 125.1, 124.5, 124.4, 122.3, 116.4, 115.6, 115.5, 115.3, 114.3, 47.6, 47.5, 31.5, 31.4, 26.9, 26.8, 26.7, 26.6, 14.0. MS (EI, 70 eV): *m/z* (relative intensity) 642 (M⁺, 100); HRMS calcd for C₃₆H₃₉N₂BrS₂: 642.1738, found 642.1741.

3-(3-Bromo-10-(4-(hexyloxy)phenyl)-10*H*-phenothiazin-7-yl)-10-(4-(hexyloxy)phenyl)-10*H*-phenothiazine (**3b**)

Compound **3b** was synthesized according to the same procedure as that of **3a**. A yellow solid of **3b** was obtained in 50% yield. δ_H (400 MHz, CDCl₃) 7.27 (dt, 2H, *J* = 8.8, 2.0 Hz), 7.23 (dt, 2H, *J* = 9.6, 2.0 Hz), 7.06–7.10 (m, 7H), 6.97 (dd, 1H, *J* = 7.6, 2.0 Hz), 6.86–6.92 (m, 3H), 6.74–6.84 (m, 2H), 6.17 (d, 2H, *J* = 6.8 Hz), 6.15 (d, 1H, *J* = 6.8 Hz), 6.01 (d, 1H, *J* = 8.8 Hz), 4.02 (t, 4H, *J* = 6.4 Hz), 1.80–1.87 (m, 4H), 1.48–1.52 (m, 4H), 1.35–1.39 (m, 8H), 0.91–0.94 (m, 6H). δ_C (100 MHz, CDCl₃) 159.0, 158.9, 144.3, 143.6, 143.0, 134.2, 133.7, 132.9, 132.5, 132.0, 131.8, 129.4, 128.6, 126.8, 126.5, 124.7, 124.5, 124.1, 122.2, 121.4, 120.0, 119.1, 116.7, 116.5, 116.4, 115.9, 115.8, 115.6, 114.1, 68.3, 31.5, 29.2, 25.7, 22.6, 14.0. MS (EI, 70 eV): *m/z* (relative intensity) 826 (M⁺, 100); HRMS calcd for C₄₈H₄₇O₂N₂BrS₂: 826.2262, found 826.2264.

10-Hexyl-7-(10-hexyl-10*H*-phenothiazin-3-yl)-10*H*-pheno-thiazine-3-carbaldehyde (**4a**)

Compound **4a** was synthesized according to the same procedure as that of **2a**. A yellow solid of **4a** was obtained in 76% yield. δ_H (400 MHz, CDCl₃) 9.80 (s, 1H), 7.64 (dd, 1H, *J* = 8.6, 2.0 Hz),

7.58 (d, 1H, $J = 2.0$ Hz), 7.31 (t, 1H, $J = 2.0$ Hz), 7.30 (d, 2H, $J = 2.0$ Hz), 7.26 (d, 1H, $J = 2.0$ Hz), 7.16 (d, 2H, $J = 8.0$ Hz), 6.93 (t, 1H, $J = 7.2$ Hz), 6.88 (d, 4H, $J = 8.4$ Hz), 3.88 (t, 2H, $J = 6.8$ Hz), 3.86 (t, 2H, $J = 6.8$ Hz), 1.81–1.85 (m, 4H), 1.44–1.48 (m, 4H), 1.30–1.35 (m, 8H), 0.93 (t, 6H, $J = 2.0$ Hz). δ_{C} (100 MHz, CDCl_3) 189.9, 150.4, 145.0, 144.4, 142.1, 135.5, 133.6, 131.0, 130.1, 128.3, 127.4, 127.3, 125.4, 125.3, 125.2, 125.2, 125.1, 124.4, 124.3, 124.0, 122.4, 116.0, 115.5, 115.3, 114.6, 48.0, 47.5, 31.5, 31.4, 26.8, 26.6, 26.5, 22.7, 22.6, 14.1, 14.0. MS (FAB, 70 eV): m/z (relative intensity) 593 ($(\text{M} + \text{H})^+$, 100); HRMS calcd for $\text{C}_{37}\text{H}_{41}\text{N}_2\text{O}_2\text{S}$: 593.2661, found 593.2674.

10-(4-(Hexyloxy)phenyl)-7-(10-(4-(hexyloxy)phenyl)-10H-phenothiazin-7-yl)-10H-phenothiazine-3-carbaldehyde (4b)

Compound **4b** was synthesized according to the same procedure as that of **2a**. An orange solid of **4b** was obtained in 82% yield. δ_{H} (400 MHz, CDCl_3) 9.68 (s, 1H), 7.44 (d, 1H, $J = 2.0$ Hz), 7.24–7.28 (m, 5H), 7.10–7.15 (m, 5H), 7.07 (d, 1H, $J = 2.4$ Hz), 6.99 (dd, 1H, $J = 7.6, 2.0$ Hz), 6.93 (dd, 2H, $J = 8.4, 2.0$ Hz), 6.79–6.84 (m, 2H), 6.19–6.22 (m, 3H), 6.16 (d, 1H, $J = 8.4$ Hz), 1.85–1.89 (m, 4H), 1.53–1.56 (m, 4H), 1.39–1.44 (m, 8H), 0.96–1.00 (m, 6H). δ_{C} (100 MHz, CDCl_3) 189.5, 149.2, 144.3, 143.8, 141.6, 135.2, 133.3, 132.8, 132.1, 132.0, 131.5, 130.8, 129.9, 127.4, 126.9, 126.6, 124.6, 124.5, 124.1, 124.0, 122.3, 120.1, 119.7, 119.4, 119.1, 116.7, 116.4, 115.8, 68.3, 31.6, 29.3, 29.2, 25.8, 22.6, 14.1. MS (FAB, 70 eV): m/z (relative intensity) 777 ($(\text{M} + \text{H})^+$, 100); HRMS calcd for $\text{C}_{49}\text{H}_{49}\text{N}_2\text{O}_3\text{S}_2$: 777.3185, found 777.3204.

10-Hexyl-7-(10-hexyl-3-(10-hexyl-10H-phenothiazin-7-yl)-10H-phenothiazin-7-yl)-10H-phenothiazine-3-carbaldehyde (5a)

Compound **5a** was synthesized according to the same procedure as that of **3a**. A yellow solid of **5a** was obtained in 65% yield. δ_{H} (400 MHz, CDCl_3) 9.81 (s, 1H), 7.66 (dd, 1H, $J = 8.4, 2.0$ Hz), 7.61 (d, 1H, $J = 2.0$ Hz), 7.31–7.34 (m, 7H), 7.28 (d, 1H, $J = 2.4$ Hz), 7.16 (d, 2H, $J = 7.6$ Hz), 6.87–6.95 (m, 7H), 3.85–3.90 (m, 6H), 1.82–1.87 (m, 6H), 1.45–1.49 (m, 6H), 1.28–1.37 (m, 12H), 0.90–0.92 (m, 9H). δ_{C} (100 MHz, CDCl_3) 189.9, 150.4, 145.1, 144.2, 143.8, 142.2, 135.5, 134.4, 134.1, 133.7, 131.0, 130.1, 128.4, 127.4, 127.2, 125.4, 125.2, 125.1, 124.8, 124.6, 124.5, 124.4, 124.1, 122.3, 116.0, 115.4, 115.3, 114.6, 48.0, 47.6, 31.4, 31.3, 26.8, 26.6, 26.5, 22.6, 22.6, 14.0. MS (FAB, 70 eV): m/z (relative intensity) 873 (M^+ , 100); HRMS calcd for $\text{C}_{55}\text{H}_{59}\text{ON}_3\text{S}_3$: 873.3820, found 873.3807.

10-(4-(Hexyloxy)phenyl)-7-(10-(4-(hexyloxy)phenyl)-3-(10-(4-(hexyloxy)phenyl)-10H-phenothiazin-7-yl)-10H-phenothiazin-7-yl)-10H-phenothiazine-3-carbaldehyde (5b)

Compound **5b** was synthesized according to the same procedure as that of **3a**. A yellow solid of **5b** was obtained in 57% yield. δ_{H} (400 MHz, CDCl_3) 9.70 (s, 1H), 7.46 (d, 1H, $J = 2.0$ Hz), 7.25–7.31 (m, 7H), 7.10–7.15 (m, 9H), 7.08 (d, 1H, $J = 2.0$ Hz), 7.00 (dd, 1H, $J = 7.2, 1.6$ Hz), 6.91–6.95 (m, 4H), 6.79–6.85 (m, 2H), 6.15–6.22 (m, 6H), 4.03–4.06 (m, 6H), 1.83–1.88 (m, 6H), 1.52–1.55 (m, 6H), 1.39–1.42 (m, 12H), 0.93–0.96 (m, 9H). δ_{C} (100 MHz, CDCl_3) 189.6, 159.3, 159.0, 158.9, 149.2, 144.4, 143.6, 143.1, 141.6, 135.2, 134.0, 133.8, 133.4, 132.9, 132.8, 132.1, 132.0, 131.5, 130.8, 129.9, 127.4, 126.8, 126.5, 124.7, 124.6, 124.5, 124.0,

122.2, 120.0, 119.78, 119.7, 119.5, 119.3, 119.2, 116.7, 116.6, 116.5, 116.4, 115.8, 115.6, 114.9, 68.4, 31.6, 29.2, 25.7, 22.6, 14.0. MS (FAB, 70 eV): m/z (relative intensity) 1149 (M^+ , 100); HRMS calcd for $\text{C}_{73}\text{H}_{71}\text{O}_4\text{N}_3\text{S}_3$: 1149.4607, found 1149.4608.

(E)-2-Cyano-3-(N-hexylphenothiazin-7-yl)acrylic acid (PT1a)

A mixture of **2a** (1.00 g, 3.21 mmol), cyanoacetic acid (355 mg, 4.17 mmol), and ammonium acetate (74 mg, 0.96 mmol) were placed in a three-necked flask in acetic acid under a nitrogen atmosphere with heating at 100 °C for 12 h. After cooling, the reaction was quenched by adding water, and extracted with CH_2Cl_2 . The organic layer was dried over anhydrous MgSO_4 and concentrated under reduced pressure to give the crude product. The product was purified using a silica gel column chromatograph eluted with CH_2Cl_2 -acetic acid (19/1). The deep red solid was isolated in 70% yield (770 mg, 1.28 mmol), mp: 154–156 °C. Spectroscopic data of **PT1a**: δ_{H} (400 MHz, DMSO-d_6) 8.14 (s, 1H), 7.90 (d, 1H, $J = 8.7$ Hz), 7.79 (d, 1H, $J = 1.7$ Hz), 7.22 (t, 1H, $J = 8.0$ Hz), 7.13–7.16 (m, 2H), 7.06 (d, 1H, $J = 8.2$ Hz), 6.99 (t, 1H, $J = 7.4$ Hz), 3.92 (t, 2H, $J = 7.2$ Hz), 1.63–1.70 (m, 2H), 1.34–1.39 (m, 2H), 1.22–1.24 (m, 4H), 0.81 (t, 3H, $J = 6.8$ Hz); δ_{C} (100 MHz, DMSO-d_6) 163.8, 152.2, 148.8, 142.7, 131.5, 129.0, 128.0, 127.3, 125.6, 123.6, 123.2, 122.1, 116.9, 116.4, 115.6, 100.0, 46.9, 30.7, 26.0, 25.7, 22.0, 13.8; MS (FAB, 70 eV): m/z (relative intensity) 378 (M^+ , 100); HRMS calcd for $\text{C}_{22}\text{H}_{22}\text{N}_2\text{O}_2\text{S}$: 378.1402, found 378.1400.

(E)-2-Cyano-3-(10-(4-(hexyloxy)phenyl)-10H-phenothiazin-7-yl)acrylic acid (PT1b)

Compound **PT1b** was synthesized according to the same procedure as that of **PT1a**. A red solid of **PT1b** was obtained in 70%, mp: 167–169 °C. δ_{H} (400 MHz, DMSO-d_6) 8.00 (s, 1H), 7.59 (s, 1H), 7.54 (d, 1H, $J = 8.8$ Hz), 7.26 (d, 2H, $J = 8.8$ Hz), 7.14 (d, 2H, $J = 8.8$ Hz), 6.95–6.97 (m, 1H), 6.84–6.86 (m, 2H), 6.17–6.20 (m, 2H), 4.06 (t, 2H, $J = 6.4$ Hz), 1.85–1.88 (m, 2H), 1.51–1.55 (m, 2H), 1.39–1.42 (m, 2H), 0.95 (t, 3H, $J = 6.8$ Hz); δ_{C} (100 MHz, DMSO-d_6) 167.9, 159.4, 154.3, 149.2, 142.3, 131.8, 131.6, 131.3, 129.4, 127.1, 126.6, 125.2, 123.8, 120.1, 118.8, 116.8, 116.6, 115.8, 115.3, 96.9, 68.4, 31.5, 29.1, 25.7, 22.6, 14.0; MS (FAB, 70 eV): m/z (relative intensity) 471 ($(\text{M} + \text{H})^+$, 100); HRMS calcd for $\text{C}_{28}\text{H}_{27}\text{N}_2\text{O}_3\text{S}$: 471.1750, found 471.1742.

(E)-2-Cyano-3-(10-hexyl-3-(10-hexyl-10H-phenothiazin-3-yl)-10H-phenothiazin-7-yl)acrylic acid (PT2a)

Compound **PT2a** was synthesized according to the same procedure as that of **PT1a**. A red solid of **PT2a** was obtained in 72%, mp: 126–128 °C. δ_{H} (400 MHz, DMSO-d_6) 8.08 (s, 1H), 7.83 (d, 1H, $J = 8.0$ Hz), 7.36 (d, 2H, $J = 8.0$ Hz), 7.32 (s, 2H), 7.14 (t, 1H, $J = 7.6$ Hz), 7.08 (d, 1H, $J = 7.2$ Hz), 7.01 (d, 1H, $J = 8.8$ Hz), 6.86–6.96 (m, 4H), 3.76–3.81 (m, 4H), 1.59–1.61 (m, 4H), 1.28–1.30 (m, 4H), 1.60–1.62 (m, 8H), 0.75–0.76 (m, 6H); δ_{C} (100 MHz, DMSO-d_6) 164.5, 151.8, 148.5, 144.8, 144.2, 141.9, 134.6, 133.1, 131.7, 129.1, 127.9, 127.5, 126.1, 125.7, 125.5, 124.7, 124.6, 123.6, 123.2, 123.1, 122.8, 117.7, 116.8, 116.2, 116.0, 115.8, 47.3, 46.9, 31.3, 31.2, 26.6, 26.4, 26.3, 26.1, 22.5; MS (FAB, 70 eV): m/z (relative intensity) 660 ($(\text{M} + \text{H})^+$, 100); HRMS calcd for $\text{C}_{40}\text{H}_{41}\text{N}_3\text{O}_2\text{S}_2$: 660.2732, found 660.2719.

(E)-2-Cyano-3-(10-(4-(hexyloxy)phenyl)-3-(10-(4-(hexyloxy)phenyl)-10H-phenothiazin-7-yl)-10H-phenothiazin-7-yl)acrylic acid (PT2b)

Compound **PT2b** was synthesized according to the same procedure as that of **PT1a**. A dark red solid of **PT2b** was obtained in 85%, mp: 172–174 °C. δ_{H} (400 MHz, DMSO- d_6) 8.02 (s, 1H), 7.71 (s, 1H), 7.54 (d, 1H, $J = 9.2$ Hz), 7.24–7.31 (m, 6H), 7.17 (d, 4H, $J = 8.0$ Hz), 7.09 (d, 2H, $J = 8.4$ Hz), 7.02 (d, 1H, $J = 6.8$ Hz), 6.88 (t, 1H, $J = 7.2$ Hz), 6.80 (t, 1H, $J = 7.2$ Hz), 6.05–6.11 (m, 4H), 4.00–4.03 (m, 4H), 1.72–1.75 (m, 4H), 1.41–1.44 (m, 4H), 1.31–1.33 (m, 8H), 0.87–0.90 (m, 6H); δ_{C} (100 MHz, DMSO- d_6) 164.2, 159.2, 158.8, 152.4, 147.5, 144.0, 143.5, 141.2, 134.4, 132.8, 132.5, 132.1, 131.8, 131.6, 131.5, 128.5, 127.5, 126.8, 125.9, 124.9, 123.9, 122.8, 119.7, 119.1, 118.9, 118.8, 117.2, 116.9, 116.1, 115.8, 115.4, 99.7, 68.2, 31.4, 29.1, 25.7, 22.5, 14.3; m/z (FAB) 844.3264 ((M + H)⁺, C₅₂H₄₉N₃O₄S₂ requires 844.3242).

(E)-2-Cyano-3-(10-hexyl-3-(10-hexyl-3-(10-hexyl-10H-phenothiazin-7-yl)-10H-phenothiazin-7-yl)-10H-phenothiazin-7-yl)acrylic acid (PT3a)

Compound **PT3a** was synthesized according to the same procedure as that of **PT1a**. A red solid of **PT3a** was obtained in 70%, mp: 112–114 °C. δ_{H} (400 MHz, THF- d_8) 8.11 (s, 1H), 8.01 (dd, 1H, $J = 8.4, 2.0$ Hz), 7.80 (d, 1H, $J = 2.0$ Hz), 7.37–7.44 (m, 8H), 6.96–7.15 (m, 8H), 6.92 (t, 1H, $J = 7.2$ Hz), 3.61–4.01 (m, 6H), 1.81–1.86 (m, 6H), 1.50–1.52 (m, 6H), 1.32–1.37 (m, 12H), 0.87–0.93 (m, 9H); δ_{C} (100 MHz, THF- d_8) 163.3, 151.9, 149.0, 145.2, 144.2, 143.9, 142.0, 135.3, 134.2, 134.1, 133.6, 130.7, 129.7, 127.0, 126.0, 125.3, 125.1, 124.9, 124.8, 124.7, 124.6, 124.0, 123.7, 122.0, 116.1, 115.9, 115.5, 115.3, 115.0, 99.8, 47.4, 47.1, 47.0, 31.5, 31.4, 26.8, 26.6, 26.4, 26.3, 22.5, 13.4; MS (FAB, 70 eV): m/z (relative intensity) 940 (M⁺, 100); HRMS calcd for C₅₈H₆₀N₄O₂S₃: 940.3878, found 940.3861.

(E)-2-Cyano-3-(10-(4-(hexyloxy)phenyl)-3-(10-(4-(hexyloxy)phenyl)-10H-phenothiazin-7-yl)-10H-phenothiazin-7-yl)acrylic acid (PT3b)

Compound **PT3b** was synthesized according to the same procedure as that of **PT1a**. A black solid of **PT3b** was obtained in 77%, mp: 152–154 °C. δ_{H} (400 MHz, THF- d_8) 8.02 (s, 1H), 7.68 (s, 1H), 7.65 (d, 1H, $J = 8.8$ Hz), 7.31–7.35 (m, 6H), 7.18–7.23 (m, 10H), 6.96–7.01 (m, 5H), 6.77–6.84 (m, 2H), 6.20–6.25 (m, 6H), 4.08 (t, 6H, $J = 6.0$ Hz), 1.83–1.88 (m, 6H), 1.56–1.58 (m, 6H), 1.41–1.43 (m, 12H), 0.97 (t, 9H, $J = 6.4$ Hz); δ_{C} (100 MHz, THF- d_8) 159.5, 159.2, 159.1, 151.5, 147.9, 144.4, 143.5, 143.1, 141.6, 133.7, 133.3, 133.0, 131.9, 131.4, 130.4, 128.9, 126.5, 126.1, 124.1, 123.6, 121.9, 120.1, 119.5, 119.3, 116.5, 116.3, 116.2, 115.7, 115.4, 115.1, 67.9, 31.59, 29.6, 29.2, 25.7, 22.5, 13.3; MS (FAB, 70 eV): m/z (relative intensity) 1216 (M⁺, 100); HRMS calcd for C₇₆H₇₂O₅N₄S₃: 1216.4665, found 1216.4678.

Quantum chemistry computations

The structure of dyes was optimized by using the B3LYP/6-31G* hybrid functional. For the excited states, a time-dependent density functional theory (TDDFT) with the B3LYP functional was employed. All analyses were performed using Q-Chem 3.0

software. The frontier orbital plots of HOMO and LUMO were drawn by using Gaussian 03.

Results and discussion

Synthesis

The key intermediate in the synthesis of **PT1**, **PT2**, and **PT3** was the *N*-substituted 7-bromophenothiazine derivatives, *i.e.*, compounds **1a** and **1b** that were prepared by *N*-alkylation. The phenothiazines with a carbaldehyde functionality (**2**, **4**, and **5**) were prepared from 10*H*-phenothiazine according to a sequence of Suzuki–Miyaura coupling¹² followed by formylation to give the products with yields of 57–82%. The presence of an aldehyde group was verified by absorption at δ 9.68–9.81 ppm in ¹H NMR. The final step was a Knoevenagel condensation between the carbaldehyde and cyanoacetic acid in the presence of ammonium acetate.¹³ The synthesis of **PT1a** was completed by a standard procedure as described in the ESI.^{†14} The structures of all new compounds were characterized by their spectroscopic data.

Absorption spectra

The UV-Vis absorption spectra of all dyes in CH₂Cl₂ solution and on TiO₂ are shown in Fig. 2 and 3, and the parameters are listed in Table 1. The compounds with multiple units of phenothiazine, *i.e.*, **PT2** and **PT3**, display longer absorption wavelengths than the mono-phenothiazine compound, *i.e.*, **PT1**. All these dyes exhibit broad absorption in the range of 250–600 nm. The short wavelength region at 250–330 nm is attributed to localized π – π^* and n – π^* transitions, while the long wavelength region in the range of 459–496 nm is derived from intramolecular charge-transfer transitions (ICT). The intensity of UV transition increases with the number of phenothiazine units, *i.e.*, **PT3** > **PT2** > **PT1**. The absorption photocurrent (J_{sc}) in maxima of ICT bands exhibits a similar trend in solutions.

The absorption spectra of all dyes absorbed on the surface of TiO₂ are shown in Fig. 3. The film absorption band displayed a blue shift of *ca.* 29–38 nm with respect to those in solutions, and the spectral difference among all dyes diminished. The blue shift appears to be a result of deprotonation of the carboxylic acid, when it is anchored onto the surface of titanium oxide.

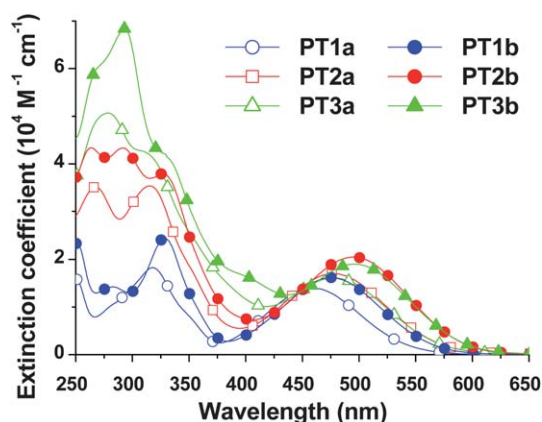
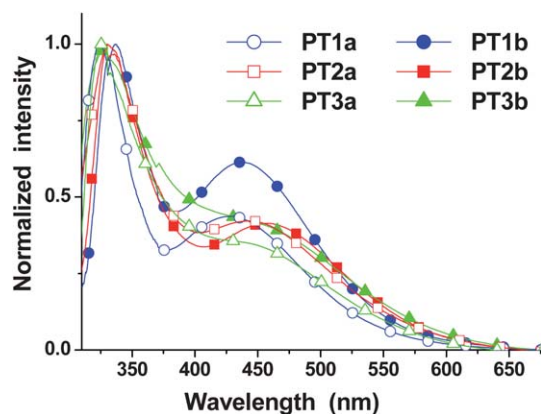


Fig. 2 Absorption spectra of dyes in CH₂Cl₂ solution.

Table 1 Photochemical and electrochemical parameters of the dyes

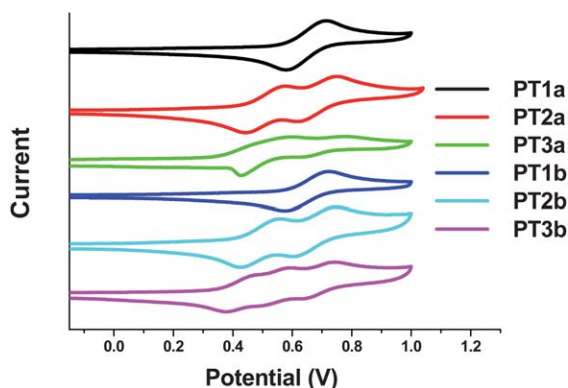
dye	λ_{\max}^a (nm)/ (ϵ ($M^{-1} \text{ cm}^{-1}$)))	Em^a (nm)	λ_{\max} (TiO_2)	E_{ox}^b (V)	E_{0-0} (eV)	E_{red}^c (V)	J_{sc} (mA cm^{-2}) E1/E2 ^e	V_{oc} (V) E1/E2	FF E1/E2	η^d (%) E1/E2
PT1a	459(14 000)	660	428	0.73	2.32	-1.59	12.91/11.03	0.68/0.76	0.62/0.65	5.45/5.43
PT2a	477(17 000)	676	448	0.59	2.24	-1.65	13.20/12.21	0.69/0.77	0.62/0.58	5.63/5.44
PT3a	478(16 100)	675	446	0.58	2.19	-1.61	12.09/10.25	0.70/0.82	0.59/0.60	5.01/5.05
PT1b	475(16 200)	655	437	0.73	2.15	-1.42	13.47/12.87	0.70/0.78	0.66/0.65	6.21/6.52
PT2b	495(20 500)	662	461	0.57	2.10	-1.53	14.48/14.00	0.71/0.82	0.61/0.64	6.30/7.38
PT3b	496(19 000)	661	459	0.50	2.03	-1.53	11.93/12.98	0.72/0.82	0.58/0.60	5.01/6.44
N719	—	—	—	—	—	—	15.87/18.61	0.74/0.76	0.61/0.63	7.15/8.93

^a Absorption and emission are in CH_2Cl_2 . ^b Oxidation potential in THF (10^{-3} M) containing 0.1 M ($n\text{-C}_4\text{H}_9$)₄NPF₆ with a scan rate of 50 mV s^{-1} (vs. NHE). ^c E_{red} calculated by $E_{\text{ox}} - E_{0-0}$. ^d Performance of DSSCs measured in a 0.25 cm^2 working area on a FTO (8Ω per square) substrate. ^e Electrolyte 1 (E1): LiI (0.5 M), I₂ (0.05 M), and TBP (0.5 M) in MeCN. Electrolyte 2 (E2): 3-dimethylimidazolium iodide (1.0 M), LiI (0.05 M), I₂ (0.03 M), guanidinium thiocyanate (0.1 M), and TBP (0.5 M) in MeCN : valeronitrile (85 : 15, v/v).

**Fig. 3** Absorption spectra of dyes absorbed on TiO_2 .

Electrochemical properties

The oxidation potentials (E_{ox}), corresponding to the highest occupied molecular orbital (HOMO) level of the dyes, were measured by cyclic voltammetry. The number of oxidative waves corresponds to the number of phenothiazine units in each compound. The lowest ionization potentials in THF solutions decreased in the order of $\text{PT1} > \text{PT2} > \text{PT3}$ (Fig. 4). It is clear that the adjacent phenothiazine moieties linked together in the same molecule can influence each other effectively. Such a conclusion is again supported by the result of theoretical

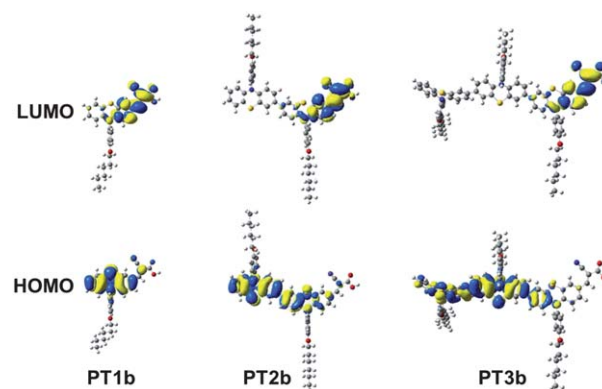
**Fig. 4** Oxidation potential of the dyes in THF (10^{-3} M).

calculations, which will be discussed in the following section. The LUMO levels of the dyes were estimated by the values of E_{ox} and the zero-zero band gaps at the onset of absorption spectra (Table 1). For a DSSCs to work properly, both the HOMO and LUMO (lowest unoccupied molecular orbital) levels have to match the conduction band (-0.5 V vs. NHE) of the TiO_2 electrode and the redox potential (0.4 V vs. NHE) of the iodine/iodide electrolyte. The energy levels of all dyes agree well with the requirements for an efficient flow of electrons.

Computational analysis

The electronic nature of the dyes was further explored by theoretical models. Full geometrical optimizations were performed by using the B3LYP/6-31G* hybrid functional implanted in Q-Chem. In the ground state the geometry of phenothiazine is not totally planar, but rather slightly bent in the center forming the shape of a butterfly. The dihedral angles are about 32° to 39° in each phenothiazine. Such a slight distortion does not seem to retard the resonance between the two fused benzene rings across the central phenothiazine moiety. As depicted in Fig. 5, the electron density in the HOMO levels of **PT2** and **PT3** spread over more than one phenothiazine unit. The strong resonance effect is beneficial to the migration of electrons upon photo-excitation.

The electron density distribution in the LUMOs of the dyes is localized mainly on the cyanoacrylate end group as shown in Fig. 5. For **PT1**, a significant electronic delocalization appears

**Fig. 5** Frontier molecular orbitals of **PT1b**, **PT2b**, and **PT3b** calculated with TDDFT (B3LYP/6-31G*) in vacuum.

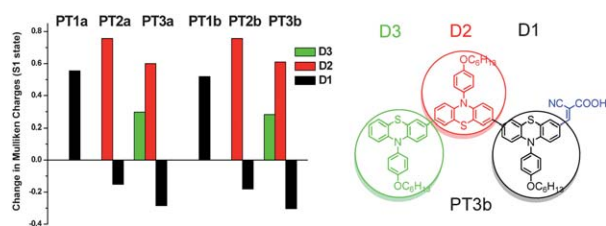


Fig. 6 Difference of Mulliken charges between ground state (S_0) and excited state (S_1), estimated by a time dependent DFT/B3LYP model.

between the cyanoacrylate and the adjacent ring in the nearest phenothiazine unit. This kind of interaction reduced the electronic density in the nearest phenothiazine unit and weakened its electron releasing property. As a result, the HOMO–LUMO energy gap in **PT1** is wider than those in **PT2** and **PT3**, therefore the ICT absorption band in the former exhibited a blue shift with respect to the latter. For **PT2** and **PT3**, there exist more than one phenothiazine units, which are all potential electron donors in ICT transitions. In **PT2** it is clear that the second phenothiazine moiety bears the most positive charge in the charge-separated state. For **PT3** the answer may not be straightforward before a quantitative analysis on the charge distribution in the excited state. In Fig. 5, a difference on Mulliken charge distributions between the ground state (S_0) and excited state (S_1) is plotted according to the estimation by the time dependent DFT/B3LYP model. From the bar chart in Fig. 6, it is clear that the second phenothiazine moiety carries most of the positive charge in the ICT state.

The bent structure of phenothiazine and its non-conjugation along the oligo-phenothiazine π -chromophores may slow down the rate of charge recombination in the excited state. The conformation of molecules is likely to be re-adjusted upon photo-excitation to accommodate the charge re-distribution along the chromophore. Any disturbance on the π -conjugation, either a distortion on molecular geometry or an interruption of the conjugation by heteroatoms, may reduce the rate of charge migration. As long as the charge-separated state can maintain a longer lifetime, a higher quantum efficiency can be achieved for the devices.

Photovoltaic performance of DSSCs

The DSSCs devices made with these dyes were fabricated according to a standard procedure. Two kinds of electrolytes were used in order to achieve the best result, *i.e.*, system E1 was made of LiI (0.5 M), I_2 (0.05 M), and TBP (4-*tert*-butylpyridine) (0.5 M) in MeCN, and system E2 was composed of 3-dimethylimidazolium iodide (DMI)(1.0 M) and guanidinium thiocyanate (0.1 M), in addition to LiI (0.05 M), I_2 (0.03 M), and TBP (0.5 M) in a mixed solvent of MeCN and valeronitrile (85 : 15, v/v). The parameters were measured under AM 1.5 solar light (100 mW cm^{-2}), *i.e.*, short-circuit current (J_{sc}), open-circuit photovoltage (V_{oc}), fill factor (FF), and solar-to-electrical photocurrent density (η) are summarized in Table 1. The photocurrent–voltage (J – V) plots of all devices are shown in Fig. 7. An apparent improvement of V_{oc} values was observed by using the new type electrolyte E2, *e.g.* an increase of *ca.* 0.10 V was obtained with respect to those using E1

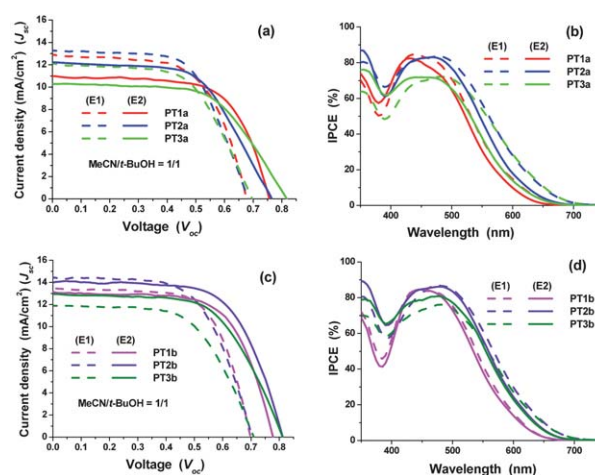


Fig. 7 J – V curves and IPCE of the DSSCs devices made with the dyes. The plots were measured under a light intensity of 1.0 sun.

(Table 1). However in all this studies, the value of J_{sc} seems to be the controlling factor on the performances. The trend of relative quantum efficiency follows the same order as the J_{sc} value, *i.e.*, **PT2** > **PT1** > **PT3**. Among all dyes, the devices made with **PT2b** performed the best, with $J_{sc} = 14.0 \text{ mA cm}^{-2}$, $V_{oc} = 0.82 \text{ V}$, and $FF = 0.64$, which summed up to an overall quantum efficiency of 7.38%.

To optimize the performance of DSSCs, it is known that the alignment of dyes on the surface of TiO_2 is a critical factor. The organic compound needs to be planted vertically on the surface of metal oxide, yet must not form aggregates of itself. It should also cover the surface as complete as possible to prevent a direct contact between TiO_2 and the electrolyte. To achieve this goal, we have made the following designs: (1) to change the electrolyte system from E1 to E2 to help preventing short-circuit and increasing the V_{oc} value. The lower concentration of LiI in E2 raises the potential level of conduction band of TiO_2 , therefore enlarges the V_{oc} value.¹⁵ (2) To add substituents with alkyl chains to reduce aggregation.¹⁶ The substituent size on the nitrogen atoms in derivatives **b** ($-C_6H_4OC_6H_{13}$) is larger than that in derivatives **a** ($-C_6H_{13}$). A long chain is able to reduce the dark current by decreasing the rate of charge recombination. The effect is supported by the higher resistance in the electrochemical impedance spectrum (EIS) of derivatives **b**.¹⁷ The V_{oc} values of derivatives **b** are considerably higher than those of derivatives **a** (Table 1). (3) To adjust the solvent used for anchoring the dyes onto TiO_2 . Among the solvents used, *i.e.*, THF, CH_2Cl_2 , EtOH– CH_2Cl_2 , and MeCN–*t*-BuOH (1 : 1), the devices made with the latter gave the best result (Fig. S22, Tables S4, and S5†). Therefore the mixed solvent system of MeCN and *t*-BuOH in 1 : 1 ratio is used for the performance parameters listed in Tables 1 and 2.

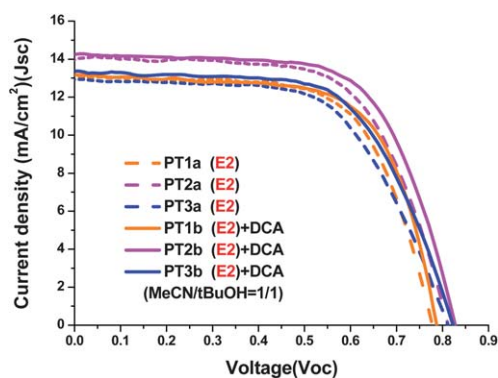
The structure of oligo-phenothiazine is not totally linear, partly due to the non-planar geometry of the phenothiazine ring, and also because of the non-symmetrical 3,7-substituted linkages between the adjacent phenothiazine moieties. The bent shape of molecules may induce some disturbance on their alignment on the surface of TiO_2 . To improve the packing order of the dyes, adding DCA (deoxycholic acid) to the solution of the dyes may

Table 2 Photovoltaic parameters of devices made **PT1b**, **PT2b** and **PT3b** with and without DCA

Dye ^a	DCA (mM)	J_{sc} (mA cm ⁻²)	V_{oc} (V)	FF	η^b (%)
PT1b	0	12.87	0.78	0.65	6.52
	10	13.03	0.80	0.67	6.98
PT2b	0	14.00	0.82	0.64	7.38
	10	14.33	0.83	0.65	7.78
PT3b	0	12.98	0.82	0.60	6.44
	10	13.33	0.83	0.62	6.87

^a Concentration of dye is 3×10^{-4} M in MeCN-*t*-BuOH (1/1).

^b Performance of DSSCs measured in a 0.25 cm² working area on an FTO (8 Ω per square) substrate under AM 1.5 condition with electrolyte 2.

**Fig. 8** Performances of DSSCs devices of **PT1b**, **PT2b**, and **PT3b** in electrolyte E2 with and without DCA.

help. As indicated in Fig. 8 and Table 2, the improvement of DCA was quite prominent, particularly for **PT2b**. The best of DSSC device exhibited a J_{sc} value 14.33 mA cm⁻², a V_{oc} value 0.83 V, and a FF value 0.66. The overall conversion efficiency (η) of **PT2b** was found to be 7.78%.

Electrochemical impedance spectroscopy

Electrochemical impedance spectroscopy (EIS) analysis was performed to further elucidate the photovoltaic property (Fig. S26 and S27†). In the Nyquist plots a major semicircle was observed for each dye, which is related to the transport process at the interfaces between TiO₂ and the electrolyte/dye.¹⁸ The charge recombination resistance at the TiO₂ surface (R_{rec}) can be deduced by fitting the curves using Z-view software. This value is related to the charge recombination rate, *e.g.*, a smaller R_{rec} indicates a faster charge recombination and therefore a larger dark current. The radius of the semicircles increase in the order of **PT1** < **PT2** < **PT3**. This trend appears to be consistent with the values of the open-circuit voltage. The electron diffuse lifetime can also be estimated in a Bode phase graph, while a shift to low frequency corresponds to a longer electron lifetime. A larger value of V_{oc} corresponds to a longer electron lifetime, while **PT2** and **PT3** have a quite high V_{oc} . The result indicated that the bent shape of phenothiazine with a long chain could prevent a direct contact between iodine and the TiO₂ surface and therefore could reduce the charge recombination rate.

Conclusions

In summary, we have successfully demonstrated that high performance DSSCs can be achieved by using the non-conjugated spacers constructed by the oligomers of phenothiazine, which act both as the electron donor and the bridge unit. In the trimer system, *i.e.*, **PT3a** and **PT3b**, the central phenothiazine ring behaved as the strongest donor, which bears most of the positive charge in the charge-separated state. The performance of the dimer system, *i.e.*, **PT2a** and **PT2b**, was better than the trimers, indicating that there exists a limiting factor on the length of the organic dyes. The promotion of V_{oc} values by the non-conjugate chromophore was clearly evidenced by the high resistance of the electrochemical impedance spectrum. The high V_{oc} values reached a level of >0.83 V, and the best conversion efficiency of 7.78% was obtained in **PT2b**. These results are also significantly better than the previous reports involving phenothiazine derivatives.^{14,19}

Acknowledgements

Financial support from the National Science Council of Taiwan and Academia Sinica are gratefully acknowledged. Special thanks to Professor C.-P. Hsu at the Institute of Chemistry for her assistance on quantum chemistry computations.

References

- B. O'Regan and M. Grätzel, *Nature*, 1999, **352**, 737.
- (a) M. K. Nazeeruddin, A. Key, I. Rodicio, R. Humphry-Baker, E. Müller, P. Liska, N. Vlachopoulos and M. Grätzel, *J. Am. Chem. Soc.*, 1993, **115**, 6382; (b) M. K. Nazeeruddin, S. M. Zakeeruddin, R. Humphry-Baker, M. Jirousek, P. Liska, N. Vlachopoulos, V. Shklover, C. H. Fischer and M. Grätzel, *Inorg. Chem.*, 1999, **38**, 6298; (c) M. K. Nazeeruddin, P. Péchy, T. Renouard, S. M. Zakeeruddin, R. Humphry-Baker, P. Comte, P. Liska, L. Cevey, E. Costa, V. Shklover, L. Spiccia, G. B. Deacon, C. A. Bignozzi and M. Grätzel, *J. Am. Chem. Soc.*, 2001, **123**, 1613; (d) M. Grätzel, *Inorg. Chem.*, 2005, **44**, 6841.
- Z. S. Wang, Y. Cui, K. Hara, Y. Dan-oh, C. Kasada and A. Shinpo, *Adv. Mater.*, 2007, **19**, 1138.
- D. Kuang, S. Uchida, R. Humphry-Baker, S. M. Zakeeruddin and M. Grätzel, *Angew. Chem., Int. Ed.*, 2008, **47**, 1923.
- S. Ko, H. Choi, M. S. Kang, H. Hwang, H. Ji, J. Kim, J. Ko and Y. Kang, *J. Mater. Chem.*, 2010, **20**, 2391.
- (a) J. J. Cid, J. H. Yum, S. R. Jang, M. K. Nazeeruddin, E. Martínez-Ferrero, E. Palomares, J. Ko, M. Grätzel and T. Torres, *Angew. Chem., Int. Ed.*, 2007, **46**, 8358; (b) C. L. Mai, W. K. Huang, H. P. Lu, C. W. Lee, Y. R. Liang, E. W. G. Diau and C. Y. Yeh, *Chem. Commun.*, 2010, **46**, 809; (c) A. Yella, H.-W. Lee, H. N. Tsao, C. Yi, A. K. Chandiran, M. K. Nazeeruddin, E. W. G. Diau, C. Y. Yeh, S. M. Zakeeruddin and M. Grätzel, *Science*, 2011, **334**, 629.
- Y. J. Chang, M. Watanabe, P.-T. Chou and T. J. Chow, *Chem. Commun.*, 2012, **48**, 726.
- (a) C. S. Krämer, K. Zeitler and T. J. J. Müller, *Tetrahedron Lett.*, 2001, **42**, 8619; (b) M. Sailer, A. W. Franz and T. J. J. Müller, *Chem.-Eur. J.*, 2008, **14**, 2602; (c) K. Memminger, T. Oeser and T. J. J. Müller, *Org. Lett.*, 2008, **10**, 2797.
- (a) H. Oka, *J. Mater. Chem.*, 2008, **18**, 1927; (b) H. Oka, *Org. Lett.*, 2010, **12**, 448; (c) T. Okamoto, M. Kuratsu, M. Kozaki, K. Hirotsu, A. Ichimura, T. Matsushita and K. Okada, *Org. Lett.*, 2004, **6**, 3493.
- (a) J. L. Segura and N. Martín, *J. Mater. Chem.*, 2000, **10**, 2403; (b) T. Otsubo, Y. Aso and K. Takimiya, *J. Mater. Chem.*, 2002, **12**, 2565; (c) E. Lukevics, P. Arsenyan and O. Pudova, *Heterocycles*, 2003, **60**, 663; (d) P. Audebert, J.-M. Catel, V. Duchenet, L. Guyard, P. Hapiot and G. Le Coustumer, *Synth. Met.*, 1999, **101**, 642.

- 11 T. Uchida, M. Ito and K. Kozawa, *Bull. Chem. Soc. Jpn.*, 1983, **56**, 577.
- 12 (a) N. Miyaura and A. Suzuki, *J. Chem. Soc., Chem. Commun.*, 1979, **19**, 866; (b) N. Miyaura and A. Suzuki, *Chem. Rev.*, 1995, **95**, 2457.
- 13 E. Knoevenagel, *Angew. Chem.*, 1922, **35**, 29.
- 14 C.-J. Yang, Y. J. Chang, M. Watanabe, Y.-S. Hon and T. J. Chow, *J. Mater. Chem.*, 2012, **22**, 4040.
- 15 (a) G. Boschloo, L. Häggman and A. Hagfeldt, *J. Phys. Chem. B*, 2006, **110**, 13144; (b) Z. Ning, Y. Fu and H. Tian, *Energy Environ. Sci.*, 2010, **3**, 1170; (c) S. A. Haque, E. Palomares, B. M. Cho, A. N. M. Green, N. Hirata and J. R. Durrant, *J. Am. Chem. Soc.*, 2005, **127**, 3456.
- 16 Z.-S. Wang, N. Koumura, Y. Cui, M. Takahashi, H. Sekiguchi, A. Mori, T. Kubo, A. Furube and K. Hara, *Chem. Mater.*, 2008, **20**, 3993.
- 17 (a) M. K. Nazeeruddin, F. De Angelis, S. Fantacci, A. Selloni, G. Viscardi, P. Liska, S. Ito, B. Takeru and M. Grätzel, *J. Am. Chem. Soc.*, 2005, **127**, 16835; (b) S. A. Haque, S. Handa, K. Peter, E. Palomares, M. Thelakkat and J. R. Durrant, *Angew. Chem., Int. Ed.*, 2005, **44**, 5740.
- 18 (a) D. Kim, M. S. Kang, K. Song, S. O. Kang and J. Ko, *Tetrahedron*, 2008, **64**, 10417; (b) N. Cho, H. Choi, D. Kim, K. Song, M. S. Kang, S. O. Kang and J. Ko, *Tetrahedron*, 2009, **65**, 6236.
- 19 (a) H. Tian, X. Yang, R. Chen, Y. Pan, L. Li, A. Hagfeldt and L. Sun, *Chem. Commun.*, 2007, 3741; (b) S. H. Kim, H. W. Kim, C. Sakong, J. Namgoong, S. W. Park, M. J. Ko, C. H. Lee, W. I. Lee and J. P. Kim, *Org. Lett.*, 2011, **13**, 5784; (c) W. Wu, J. Yang, J. Hua, J. Tang, L. Zhang, Y. Long and H. Tian, *J. Mater. Chem.*, 2010, **20**, 1722; (d) M. Marszalek, S. Nagane, A. Ichake, R. Humphry-Baker, V. Paul, S. M. Zakeeruddin and M. Grätzel, *J. Mater. Chem.*, 2012, **22**, 889; (e) C. Chen, J.-Y. Liao, Z. Chi, B. Xu, X. Zhang, D.-B. Kuang, Y. Zhang, S. Liu and J. Xu, *J. Mater. Chem.*, 2012, **22**, 8994; (f) T. Meyer, D. Ogermann, A. Pankrath, K. Kleinermanns and T. J. J. Müller, *J. Org. Chem.*, 2012, **77**, 3704.